Parametric Study on the Failure of Fiber-Reinforced Composite Laminates under Biaxial Tensile Load

WEN-PIN LIN*
Department of Civil Engineering
Chinese Military Academy
P.O. Box 90602-6, Fengshan
Taiwan 830, R.O.C.

HSUAN-TEH HU
Department of Civil Engineering
National Cheng Kung University
1 University Road, Tainan
Taiwan 701, R.O.C.

(Received March 11, 2001)
(Revised November 16, 2001)

ABSTRACT: A numerical constitutive model for a single layer of fiber-reinforced composite laminates, including nonlinear stress–strain relations, mixed failure criterion and post failure response, is used to predict the ultimate strengths of the composite laminates under biaxial tensile loads. The nonlinear constitutive law uses a variable shear parameter to model the nonlinear behavior of the in-plane shear. The onset of failure for individual lamina is determined by a mixed failure criterion composed of the Tsai-Wu and the maximum stress criteria. After the initial damage occurs, the response of the lamina is described by brittle or degrading modes up to the collapse of the entire laminate. The constitutive model is tested against experimental data and satisfactory results are obtained. In addition, parametric studies for composite laminates with different laminate layups and under various biaxial tensile load ratios are presented.

KEY WORDS: nonlinear constitutive law, nonlinear shear parameter, mixed failure criterion, post failure response, biaxial tensile load, laminate layups.

INTRODUCTION

THE BEHAVIOR OF fiber-reinforced plastic materials is complicated by the fact that it is not only anisotropic, but, on the macro scale, is also inhomogeneous. These properties

*Author to whom correspondence should be addressed. E-mail: wplin@cc.cma.edu.tw

0021-9983/02/12 1481–23 $10.00/0 DOI: 10.1106/002199802023218

cause a variety of failure mechanisms associated with fiber-reinforced composite materials. For example, when a composite material is subjected to loading, the matrix can develop cracks, plies may delaminate, or fibers can debond from the matrix and fail. This damage leads to a localized or global failure of the composite material involving one or more of many failure modes possible. The study of the failure modes and damage propagation is an integral part of the characterization of composite materials.

Materials in practical structures are usually subjected to biaxial or triaxial stresses. These structures include pressure vessels, pipes, drive shafts and rocket motors, etc. As the use of composite materials under such complex loading conditions has increased, so has the need for reliable design criteria which can be easily manipulated by the design engineer with reasonable accuracy.

Filament wound composite tubes have been the subject of numerous experimental investigations. Biaxial testing of tubes has evolved from the three basic tests, i.e., axial load, internal pressure and pressure vessel type loading where the ratio of hoop stress to axial stress is 2 : 1. Due to the development of biaxial testing systems, it is possible to conduct biaxial tests at any ratio of internal pressure to axial load [1–6]. In addition to the experimental work, several theoretical predictions on the failure of composite laminates under biaxial stress have been presented [7–16].

The objective of this investigation is to test the constitutive model proposed by the authors [17] against experimental data of composite tubes [3] to verify the accuracy of this model in modeling the behaviors of composite laminates subjected to biaxial loads. Then parametric studies for composite laminates with different laminate layups (including symmetric angle-ply and symmetric cross-ply laminates) and under various biaxial tensile load ratios are carried out. Finally, the influence of those parameters (laminate layups and biaxial tensile load ratios) on the stress–strain curve, failure stress and the failure envelope of composite laminates under various biaxial loads are studied and discussed.

NONLINEAR ANALYSIS MODEL

Idealized Stress–Strain Curve and Post Damage Model

For a single lamina under loading, the stress–strain curves of the proposed nonlinear analysis model are shown in Figure 1. The model comprises two basic regions in fiber and matrix; namely, the elastic and post-damage regions. And, it comprises two basic regions in in-plane shear; namely, the nonlinear and post-damage regions. For the present model, it is assumed that the material response can be adequately represented by linear stress–strain curves in the principal material directions, 1-direction (fiber direction) and 2-direction (transverse direction) of the lamina, and by a nonlinear stress–strain curve for in-plane shear in 1-2 direction. During the nonlinear stage in shear direction, the nonlinear shear modulus, G_{12n}, is dependent on the shear strain, γ_{12}. In the pre-damage regions, the elastic modulus is denoted by E_{ii} $(i = 1, 2)$ in the principal material directions. In the post-damage region, the elastic stiffnesses are dropped to zero (brittle modes) in 1-direction and 1-2 direction. However, the elastic stiffness is assumed to have a negative modulus E_{22f} (degrading mode) in 2-direction. This means that the damaged lamina unloads in the transverse direction through a negative tangent modulus until no load remains in the lamina.

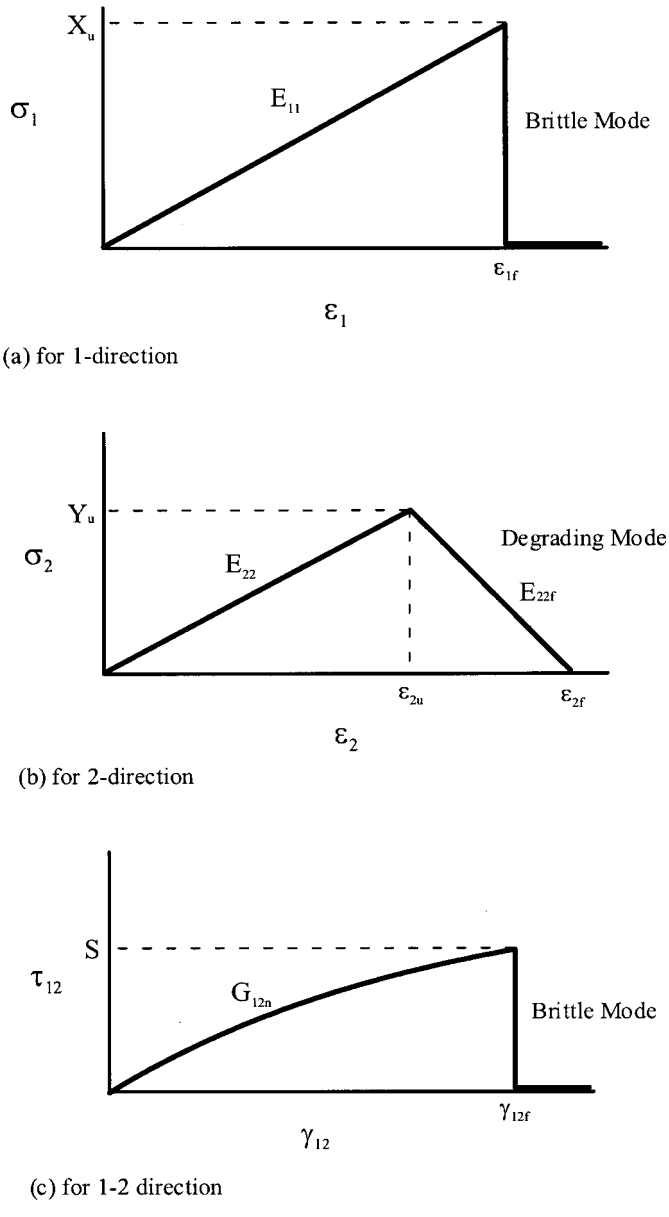

Figure 1. *Stress–strain curves of the proposed nonlinear failure model: (a) for 1-direction, (b) for 2-direction, (c) for 1-2 direction.*

Nonlinear Constitutive Model of a Lamina

For fiber-composite laminate materials, each lamina can be considered as an orthotropic layer in a plane stress condition. Taking into account the elastic-plastic behaviors in the 1-direction and 2-direction and the nonlinear behavior on the 1-2 plane within

the lamina, the stress–strain relations for an orthotropic lamina in the material coordinates $(1, 2)$ can be written as [18]

$$\begin{Bmatrix} \varepsilon_1 \\ \varepsilon_2 \\ \gamma_{12} \end{Bmatrix} = \begin{bmatrix} \frac{1}{E_{11}} & \frac{-\nu_{21}}{E_{22}} & 0 \\ \frac{-\nu_{12}}{E_{11}} & \frac{1}{E_{22}} & 0 \\ 0 & 0 & \frac{1}{G_{12}} \end{bmatrix} \begin{Bmatrix} \sigma_1 \\ \sigma_2 \\ \tau_{12} \end{Bmatrix} + S_{6666}\tau_{12}^2 \begin{Bmatrix} 0 \\ 0 \\ \tau_{12} \end{Bmatrix} \tag{1}$$

where $\varepsilon_1, \varepsilon_2$, and γ_{12} represent the strains in 1-direction, 2-direction and 1-2 plane, respectively. σ_1, σ_2 and τ_{12} denote the stresses in 1-direction, 2-direction and 1-2 plane, respectively. The terms ν_{12} and ν_{21} are the Poisson's ratios. The terms E_{11} and E_{22} are the elastic moduli in 1-direction and 2-direction. G_{12} is the shear modulus and S_{6666} is a shear parameter to account for the in-plane shear nonlinearity. The S_{6666} is a function of shear strain and can be determined by fitting the stress–strain curve of pure shear test data.

The incremental stress–strain relations for a nonlinear orthotropic lamina can be given as follows:

$$\Delta\{\sigma'\} = [Q_1']\Delta\{\varepsilon'\} \tag{2}$$

$$\Delta\{\tau_l'\} = [Q_2']\Delta\{\gamma_l'\} \tag{3}$$

where $\Delta\{\sigma'\} = \Delta\{\sigma_1, \sigma_2, \tau_{12}\}^T$, $\Delta\{\tau_l'\} = \Delta\{\tau_{13}, \tau_{23}\}^T$, $\Delta\{\varepsilon'\} = \Delta\{\varepsilon_1, \varepsilon_2, \gamma_{12}\}^T$, $\Delta\{\gamma_l'\} = \Delta\{\gamma_{13}, \gamma_{23}\}^T$, and

$$[Q_1'] = \begin{bmatrix} \frac{E_{11}}{1-\nu_{12}\nu_{21}} & \frac{\nu_{12}E_{22}}{1-\nu_{12}\nu_{21}} & 0 \\ \frac{\nu_{21}E_{11}}{1-\nu_{12}\nu_{21}} & \frac{E_{22}}{1-\nu_{12}\nu_{21}} & 0 \\ 0 & 0 & \frac{1}{1/G_{12} + 3S_{6666}\tau_{12}^2} \end{bmatrix} \tag{4}$$

$$[Q_2'] = \begin{bmatrix} \alpha_1 G_{13} & 0 \\ 0 & \alpha_2 G_{23} \end{bmatrix} \tag{5}$$

The terms α_1 and α_2 are the shear correction factors and are taken to be 0.83 in this study [19]. It is assumed that the transverse shear stresses always behave linearly and do not affect the nonlinear in-plane behavior of individual lamina.

FAILURE CRITERION AND DEGRADATION OF STIFFNESS

Mixed Failure Criteria

The Tsai-Wu failure criterion has a general nature because this failure criterion contains almost all other polynomial theories as special cases. But in some cases, the predictions of

the Tsai-Wu criterion are unreasonable due to the predicted failure stress in fiber exceeding the strength of material. In order to eliminate this unreasonable phenomenon, the limitation of maximum stress of fiber is added into the Tsai-Wu failure criterion to obtain a mixed failure criterion [17]. Under the plane stress condition, the mixed failure criterion is written in the following form:

$$F_1\sigma_1 + F_2\sigma_2 + F_{11}\sigma_1^2 + 2F_{12}\sigma_1\sigma_2 + F_{22}\sigma_2^2 + F_{66}\tau_{12}^2 = 1 \tag{6}$$

and

$$\frac{\sigma_1}{X_{ut}} = 1 \tag{7}$$

where

$$F_1 = \frac{1}{X_{ut}} + \frac{1}{X_{uc}}, \quad F_{11} = \frac{1}{X_{ut}X_{uc}}, \quad F_2 = \frac{1}{Y_{ut}} + \frac{1}{Y_{uc}}, \quad F_{22} = \frac{1}{Y_{ut}Y_{uc}}, \quad F_{66} = \frac{1}{S^2}.$$

The X_{ut}, Y_{ut} and X_{uc}, Y_{uc} are the lamina longitudinal and transverse ultimate strengths in tension and compression, respectively, and S is the shear strength of the lamina. Though the stress interaction term F_{12} in Equation (6) is difficult to be determined, it has been suggested by Narayanaswami and Adelman [20] that F_{12} can be set equal to zero for practical engineering applications. Therefore, $F_{12} = 0$ is used in this investigation.

Property Degradation Models

Material degradation within the damaged area was evaluated based on the mode of failure predicted by the failure criteria. Therefore, the residual stiffnesses of composites greatly depend on the mode of failure in each layer. The property degradation models for each layer can be separated into three idealized types of failure modes named as brittle, ductile and degrading [21,22]. For the brittle mode, the material is assumed to lose its entire stiffness and strength in the dominant stress direction, whereas for the ductile mode the material retains its strength but loses all of its stiffness in the failure direction. And, for the degrading mode the material is assumed to lose its stiffness and strength gradually in the failure direction. In this investigation, the post failure modes are idealized as the brittle behavior for σ_1 and τ_{12} and as the degrading behavior for σ_2 [17].

In the mixed failure theory, since this failure criterion can not distinguish failure modes, the following three rules are used to determine whether the ply failure is caused by matrix fracture, shear failure, or fiber breakage or buckling [23]:

(1) If a layer fails in the condition of $X_{uc} < \sigma_1 < X_{ut}$ and $-S < \tau_{12} < S$, the failure is assumed to be matrix induced. Consequently, the degradation of transverse stiffness occurs. Due to the interlock action with the neighboring plies, the damaged layer gradually loses its capability to support transverse stress, until the fracture in shear or the

breakage or buckling in fiber on the same layer. But, the lamina remains to sustain the longitudinal and shear stresses. In this case, the constitutive matrix of the lamina becomes

$$\left[D_1^{'}\right] = \begin{bmatrix} E_{11} & 0 & 0 \\ 0 & E_{22f} & 0 \\ 0 & 0 & G_{12n} \end{bmatrix} \tag{8}$$

where E_{22f} is a negative tangent modulus in transverse direction of the damaged layer, and

$$G_{12n} = \frac{1}{1/G_{12} + 3S_{6666}\tau_{12}^2}.$$

The term G_{12n} represents the nonlinear shear modulus.

(2) If the ply fails in the condition of $X_{uc} < \sigma_1 < X_{ut}$, and $\tau_{12} \geq S$ or $\tau_{12} \leq -S$, the failure is assumed to be shear induced. Consequently, the damaged lamina loses its capability to support transverse and shear stresses, but remains to carry longitudinal stress. In this case, the constitutive matrix of the lamina becomes

$$[D_1'] = \begin{bmatrix} E_{11} & 0 & 0 \\ 0 & 0 & 0 \\ 0 & 0 & 0 \end{bmatrix} \tag{9}$$

(3) If the ply fails with $\sigma_1 \geq X_{ut}$ or $\sigma_1 \leq X_{uc}$, the ply failure is caused by the fiber breakage or buckling and a total ply rupture is assumed. Thus, the constitutive matrix of the lamina becomes

$$[D_1'] = \begin{bmatrix} 0 & 0 & 0 \\ 0 & 0 & 0 \\ 0 & 0 & 0 \end{bmatrix} \tag{10}$$

LAMINATE GOVERNING EQUATIONS

The foregoing nonlinear failure model for fiber-reinforced composite laminates can be combined with classical lamination theory to form the following incremental laminate force–strain relations:

$$\Delta\{N\} = \sum_{i=1}^{m} [D]_i h_i \Delta\{\varepsilon\} \tag{11}$$

where $\Delta\{N\} = \Delta\{N_x, N_y, N_{xy}\}^T$ and $\Delta\{\varepsilon\}$ represent the vectors of the resultant membrane forces and the incremental strains in the overall laminate coordinate system (x, y), respectively. The term h_i denotes the thickness of the ith layer, m is the number of layers.

The stiffness matrix $[D]_i$ stands for elastic, elastoplastic and post-failure constitutive matrices, whichever is applicable, for the ith layer.

NUMERICAL ANALYSIS

General Description

The aforementioned nonlinear constitutive model combined with mixed failure criterion and post failure mode for composite materials are implemented into a FORTRAN subroutine and linked to the ABAQUS finite element program [24]. The analyzed laminates are simply supported around all edges of the plate as shown in Figure 2. The ply orientation of the laminate can be selected arbitrarily, but it must be symmetric with respect to the middle plane of the plate. The laminate is subjected to biaxial tensile load. The aspect ratios of all laminates analyzed are $L/W = 1$ with $t/W < 1/20$, where L, W and t represent the length, width and thickness of the laminate, respectively. The laminae are assumed to be perfectly bounded and no slipping occurs within the laminate. Since the stress field is uniform throughout the composite, only one quadrangular shell element with eight nodes is used to simulate the laminate in the numerical analysis.

In ABAQUS program, the local stresses and strains of the shell element in each lamina within the laminate can be automatically transformed to global coordinates. Basically, stresses and strains are calculated at each incremental step, and evaluated by the failure criteria to determine the occurrence of failure and the mode of failure. Mechanical properties in the damage area are reduced appropriately, according to the property degradation models. Stresses and strains will then be recalculated to determine any additional damage as a result of stress redistribution at the same load. This procedure will continue until no additional damage is found, and the next increment is then pursued.

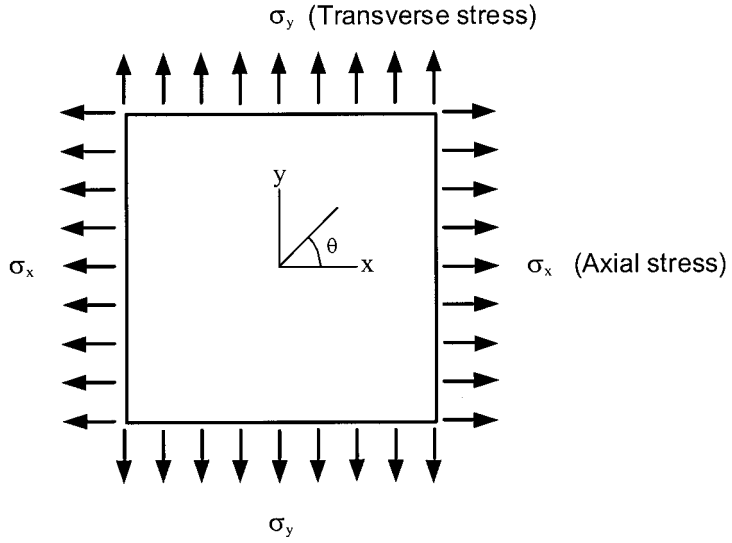

Figure 2. *Geometry and biaxial tensile load on the composite laminate.*

The final collapse load is determined when the composite plates cannot sustain any additional load.

The material used in the numerical analysis is E-Glass/epoxy composites. Its material properties and strengths are [25]:

1. Material properties:

$E_{11} = 45.6\,\text{GPa},\ E_{22} = 16.2\,\text{GPa},\ E_{22f} = -4.02\,\text{GPa},\ G_{12} = 5.83\,\text{GPa},\ \nu_{12} = 0.278$

$$S_{6666} = \left\{ \begin{array}{l} 0\,\text{GPa}^{-3}, \text{if } 0 \le \gamma_{12} \le 0.006 \\ 9723.85(\gamma_{12} - 0.006)\,\text{GPa}^{-3}, \textit{if } 0.006 \le \gamma_{12} \le 0.007 \\ -3.56942 + 1899.03882\gamma_{12}\text{GPa}^{-3}, \textit{if } 0.007 \le \gamma_{12} \le 0.04 \end{array} \right\}$$

2. Ultimate strengths:

$X_{ut} = 1280\,\text{MPa},\ X_{uc} = -800\,\text{MPa},\ Y_{ut} = 40\,\text{MPa},\ Y_{uc} = -145\,\text{MPa},\ S = 72\,\text{MPa}.$

The variable shear parameter, S_{6666}, is obtained by curve fitting from the pure shear test data [25], as shown in Figure 3.

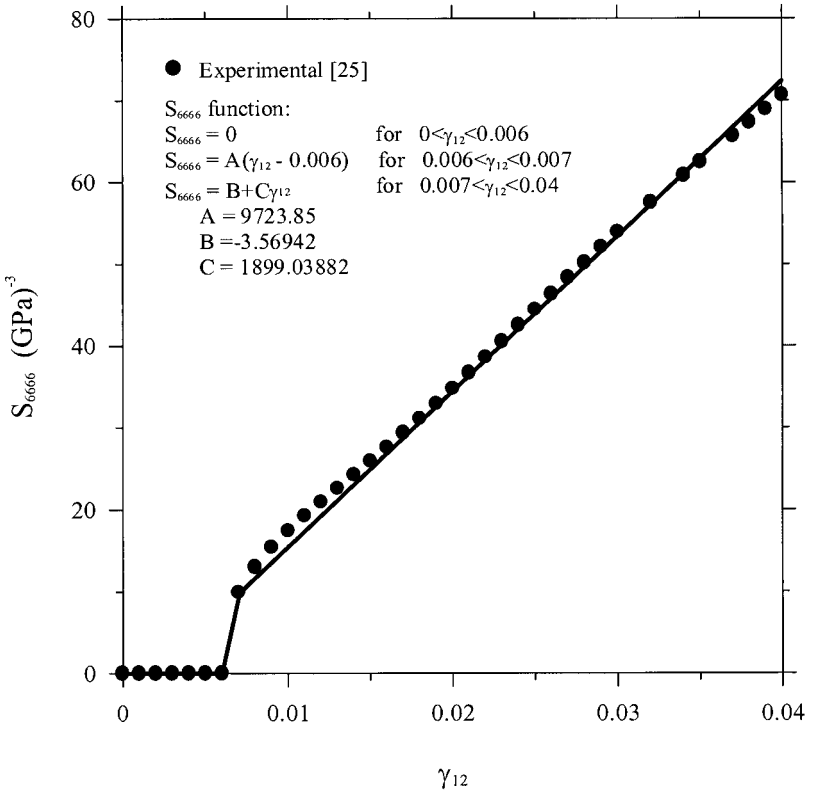

Figure 3. *Nonlinear shear parameter S_{6666} vs. shear strains γ_{12} for E-glass/MY750/HY917/DY063 epoxy lamina.*

Validation of the Proposed Nonlinear Analysis Model

The proposed nonlinear constitutive model has been shown to be a reasonable and accurate approach in the nonlinear failure analysis of fiber-reinforced composite laminated materials subjected to uniaxial loading [17]. To verify this constitutive model also suitable for the failure analysis on fiber-reinforced composite laminated materials subjected to biaxial loading, the predictions obtained by the proposed model are compared with experimental data [3] and with the predictions obtained by other analysis models. Two analysis models, the stress-based Grant-Sanders method used by Edge [9] and the progressive failure model developed by Liu and Tsai [14], are selected to compare with the proposed analysis model. The stress-based Grant-Sanders method is based on a ply-by-ply analysis with discrete failure criteria; the only interactions considered being shear-tension for matrix failure and shear-compression for fiber failure. The progressive failure model is also based on a ply-by-ply analysis but using the degrading factors to modify the stiffness and strength of fiber and matrix in damaged zone, and uses the Tsai-Wu failure criterion to determine the failure onset of individual lamina within the laminate. Figure 4 illustrates the failure envelope for $[+55/-55]_S$

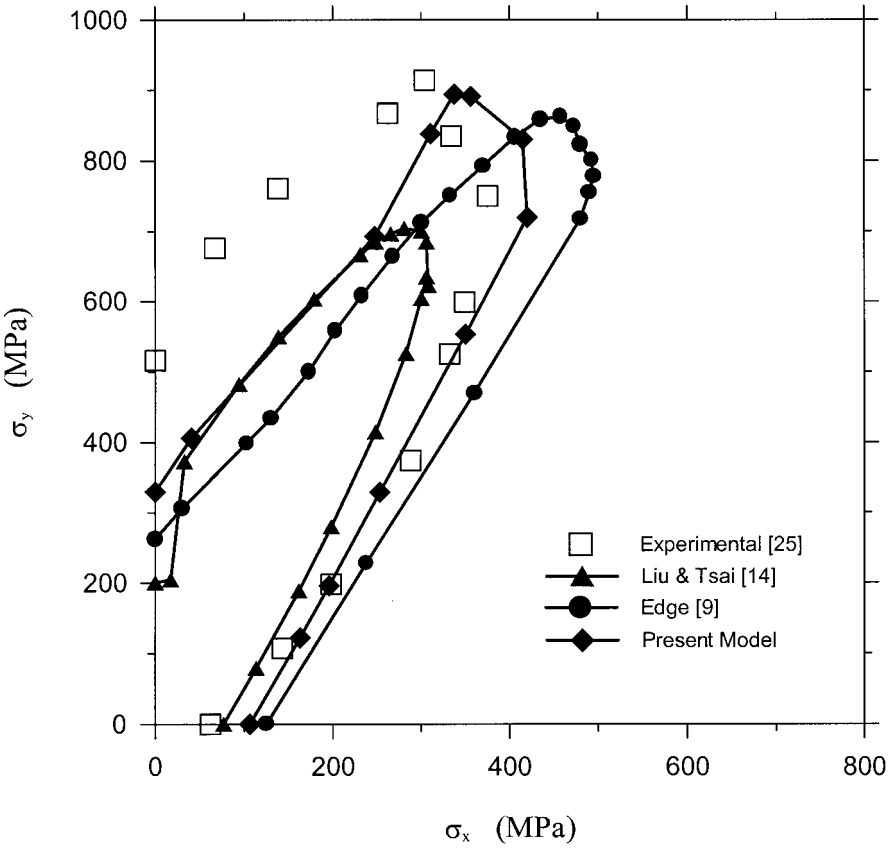

Figure 4. *Failure envelopes for* $[+55/-55]_S$ *laminate under biaxial tensile loads.*

E-glass/epoxy laminates under various biaxial tensile loads. It shows the predictions obtained by the proposed constitutive model have a better agreement with the experimental data [3] than those predicted by Liu and Tsai [14] and Edge [9]. Thus, the proposed nonlinear analysis model is reasonably accurate in predicting the failure behavior of fiber-reinforced composite laminates under biaxial loading.

Parametric Investigation

Two major parameters, biaxial tensile stress ratio and laminate layup, are concerned in this study. The biaxial stress ratio is defined as the ratio of axial stress to transverse stress of laminate, i.e., $SR = \sigma_x/\sigma_y$. The laminate layups include two types of laminate, i.e., symmetric angle-ply laminate $[\pm\theta]_S$ and symmetric cross-ply laminate $[\theta/(\theta - 90)]_S$. The influences of these two parameters on the behavior of composite laminates under biaxial tensile loading are investigated as follows.

$[\pm\theta]_S$ LAMINATES

In this section, first, the influence of biaxial stress ratio on the stress–strain curve of a given $[\pm\theta]_S$ laminate is investigated. The $[\pm\theta]_S$ laminates include $[0/0]_S$, $[+15/-15]_S$, $[+30/-30]_S$, and $[+45/-45]_S$ layups. Then, the stress–strain behaviors of various $[\pm\theta]_S$ laminates under a special biaxial stress ratio, $SR = 1/1$, are investigated. Finally, the influence of laminate layup on the failure stress and the failure envelope of composite laminates under biaxial stress are studied.

Figures 5–8 illustrate the stress–strain curves for various $[\pm\theta]_S$ laminates under various biaxial tensile loads. For $[0/0]_S$ laminate subjected to uniaxial tensile load ($SR = 1/0$), the stress–strain curve (Figure 5) is linear due to the deformation of laminate dominated by fiber and the failure dominated by fiber breakage. If a small transverse tensile load is added into the laminate to generate a biaxial stress state, say $\sigma_y = 0.04\sigma_x$ ($SR = 1/0.04$), it changes the failure mode from fiber breakage to matrix tensile cracking failure and decreases the axial failure stress of the laminate. This means that the failure mode of the laminate is changed from fiber failure dominant to matrix cracking failure dominant. As the transverse stresses increase, the axial failure stresses of laminate decrease rapidly. Under these load conditions, the $\sigma_x - \varepsilon_x$ curves remain linear and keep the same slope as the original curve without any transverse load acting on it ($SR = 1/0$). However, the $\sigma_x - \varepsilon_y$ curves change their slopes gradually due to the fact that the tensile transverse strains increase with the transverse tensile loading. As the biaxial stress ratio decreases from $SR = 1/0$ down to $SR = 1/1$, the failure of laminate is fully dominated by matrix. It is noted that no initial failure occurs for $[0/0]_S$ laminate.

For $[+15/-15]_S$ laminate (Figure 6), $\sigma_x - \varepsilon_x$ curve is nearly linear under uniaxial tensile load ($SR = 1/0$), but the failure mode is coupled by fiber failure and shear failure. If a small transverse tensile load is added into the laminate to generate a biaxial stress state, say $\sigma_y = 0.04\sigma_x$, it changes the failure mode from the coupled fiber and shear failures to shear failure only and the axial failure stress of the laminate is decreased. As the transverse stress increases, the axial failure stress of laminate decreases rapidly and the failure mode of laminate changes to matrix cracking failure. When the biaxial stress ratio decreases from $SR = 1/0$ down to $SR = 1/0.1$, the failure of laminate is fully dominated by matrix. Again no initial failure occurs for $[+15/-15]_S$ laminate.

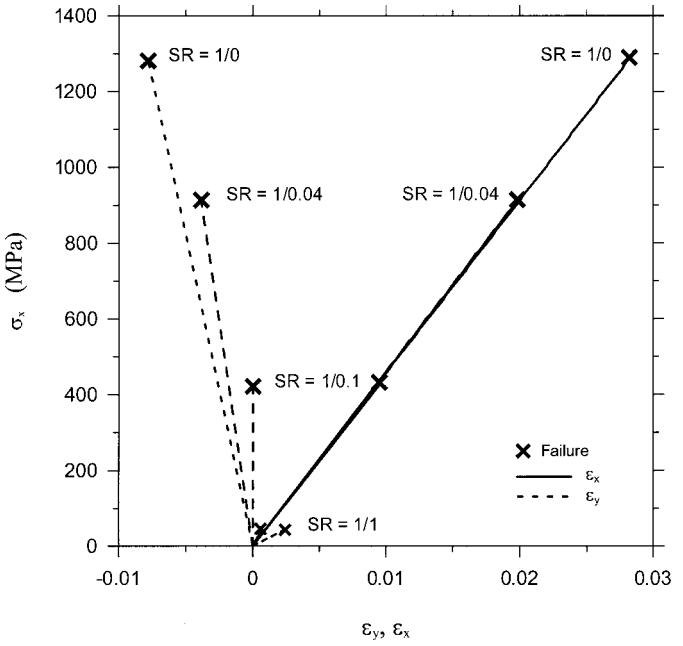

Figure 5. *Stress–strain curves for $[0/0]_S$ laminate under various biaxial tensile loads.*

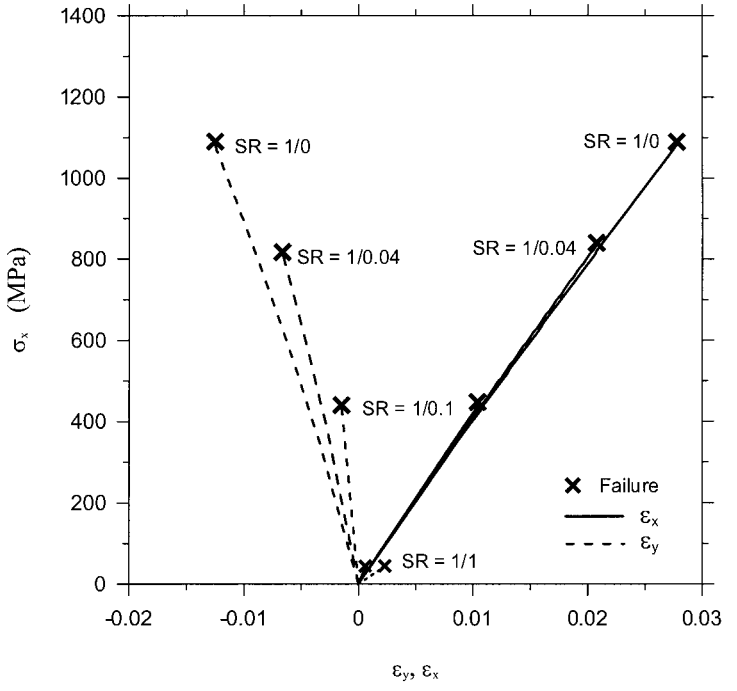

Figure 6. *Stress–strain curves for $[+15/-15]_S$ laminate under various biaxial tensile loads.*

For $[+30/-30]_S$ laminate (Figure 7), the stress–strain curve of the laminate under uniaxial tensile load ($SR = 1/0$) is nonlinear due to the behavior of laminate being dominated by shear deformation and the failure mode of the laminate is shear failure. If a small transverse tensile load is added into the laminate to generate a biaxial stress state, say $\sigma_y = 0.04\sigma_x$ ($SR = 1/0.04$), it enhances the nonlinear shear behavior of the laminate and increases the axial failure stress of the laminate. This phenomenon is valid up to the case $\sigma_y = 0.1\sigma_x$ ($SR = 1/0.1$). As $\sigma_y > 0.1\sigma_x$, the failure mode of laminate gradually changes from the shear failure dominant to matrix cracking failure dominant, and the axial failure stress decreases rapidly. Under the biaxial load with $SR = 1/1$, the transverse strain ε_y changes from negative to positive and is greater than the axial strain, ε_x, due to the weakness in transverse direction of laminate. Hence, the laminate fails with matrix cracking at a very lower stress. Under $SR = 1/1$, the laminate initiates matrix cracking (initial failure) on 30 and -30° plies simultaneously, and finally has matrix failure (final failure) on both type plies at the same time.

For $[+45/-45]_S$ laminate (Figure 8), the stress–strain curve of the laminate under uniaxial tensile load ($SR = 1/0$) is nonlinear due to the behavior of laminate dominated by shear deformation. If a transverse tensile load is added into the laminate to generate a biaxial stress state, say $\sigma_y = 0.5\sigma_x$ ($SR = 1/0.5$), it decreases the nonlinear response of the laminate and increases the axial failure stress of the laminate. If the biaxial stress ratio increases to $SR = 1/1$, the stress–strain curves, σ_x–ε_x and σ_x–ε_y curves, change into the same bilinear form due to the behavior of laminate dominated by fiber deformation and having the same stress–strain response in x and y directions. For this type of laminate, the

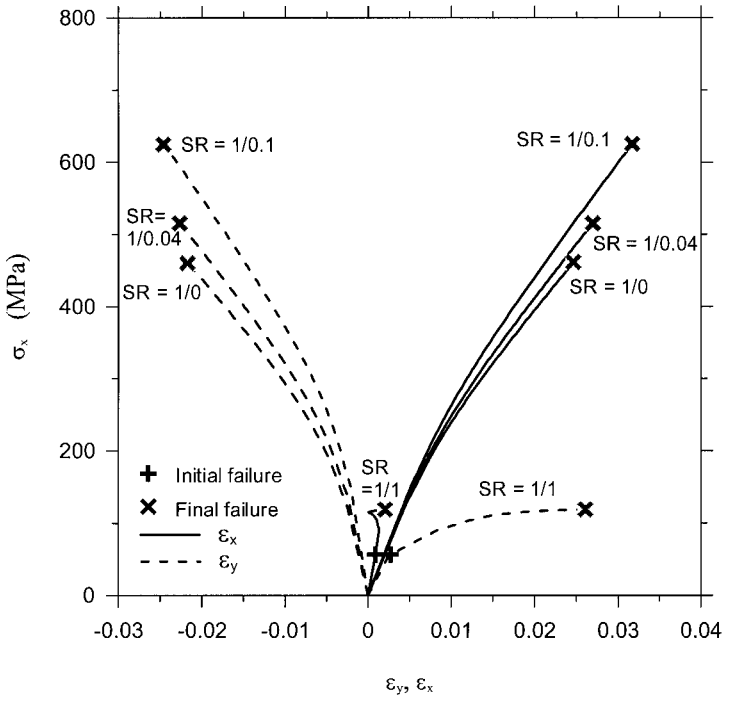

Figure 7. *Stress–strain curves for $[+30/-30]_S$ laminate under various biaxial tensile loads.*

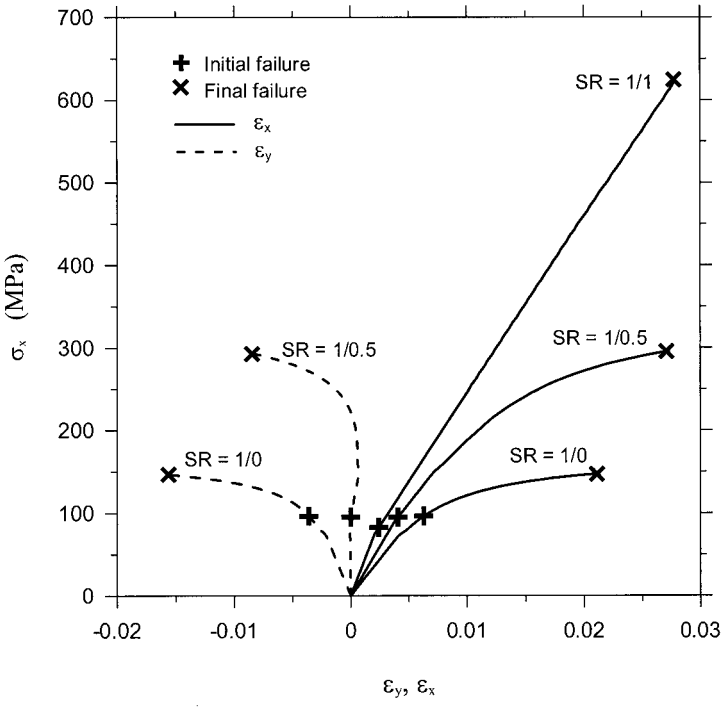

Figure 8. *Stress–strain curves for [+45/ −45]$_S$ laminate under various biaxial tensile loads.*

initial matrix cracking occurs on 45 and −45° plies simultaneously (initial failure), and finally the fiber breaks on both plies at the same time (final failure). The axial final failure stress increases as SR changes from 1/0 to 1/1, but the initial failure stresses are nearly the same for different biaxial stress ratios. The initial failure mode is matrix cracking, but the final failure mode is fiber failure for all the biaxial stress ratios.

Figure 9 shows the stress–strain curves for various $[\pm\theta]_S$ laminates under biaxial tensile load with $SR = 1/1$. In the figure, only the curves with $30° \leq \theta \leq 60°$ are plotted. For θ beyond this region, the curves are either too close to the curve of $[\pm 30]_S$ layup or too close to the curve of $[\pm 60]_S$ layup to distinguish the difference. Due to symmetry, the σ_x–ε_y curves of $[\pm 30]_S$, $[\pm 35]_S$ and $[\pm 40]_S$ laminates are the same as the σ_x–ε_x curves of $[\pm 60]_S$, $[\pm 55]_S$ and $[\pm 50]_S$ laminates and the σ_x–ε_y curves of $[\pm 60]_S$, $[\pm 55]_S$ and $[\pm 50]_S$ laminates are the same as the σ_x–ε_x curves of $[\pm 30]_S$, $[\pm 35]_S$ and $[\pm 40]_S$ laminates. For $[\pm 30]_S$, $[\pm 35]_S$ and $[\pm 40]_S$ laminates, the transverse strains increase more rapidly than the axial strains do as the stress increases. Due to the effect of the Poisson's ratio, the axial strain starts to decrease near the ultimate failure load. The axial failure stress of $[\pm\theta]_S$ laminate increases as θ increases from 0 to 45° and decreases as θ increases from 45 to 90°. The axial failure stress of $[\pm 45]_S$ laminate is the largest among various $[\pm\theta]_S$ laminates.

Figure 10 illustrates the axial failure stresses, σ_{xf}, for various $[\pm\theta]_S$ laminates under different biaxial tensile loads. It shows the axial failure stress of $[\pm\theta]_S$ laminate changes with θ for certain biaxial stress ratio. There exists an optimum θ at which the maximum axial failure stress reaches. For example, the optimum θ for $SR = 1/0$, $SR = 1/1$ and $SR = 1/2$ are 0, 45 and 55°, respectively. Generally, the optimal angle θ increases with the

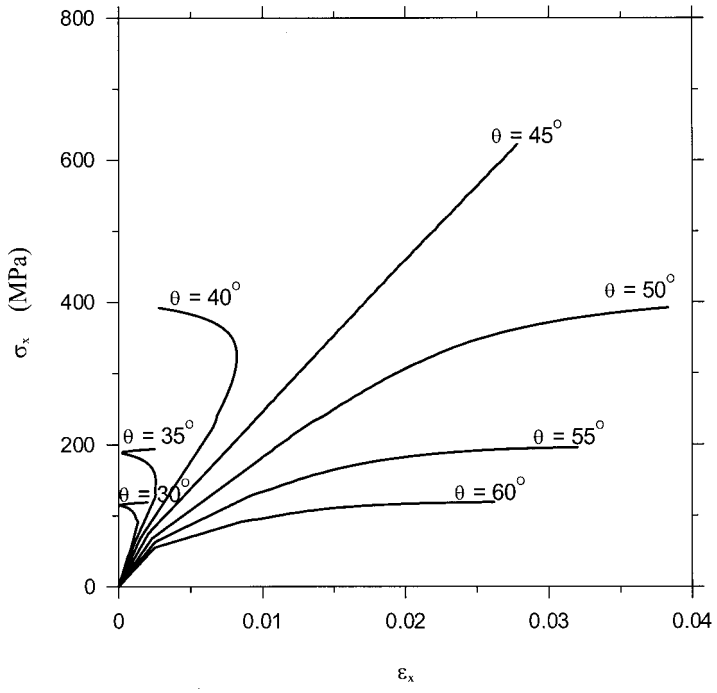

Figure 9. *Stress–strain curves for various* $[+\theta/-\theta]_S$ *laminates under biaxial tensile load with SR = 1/1.*

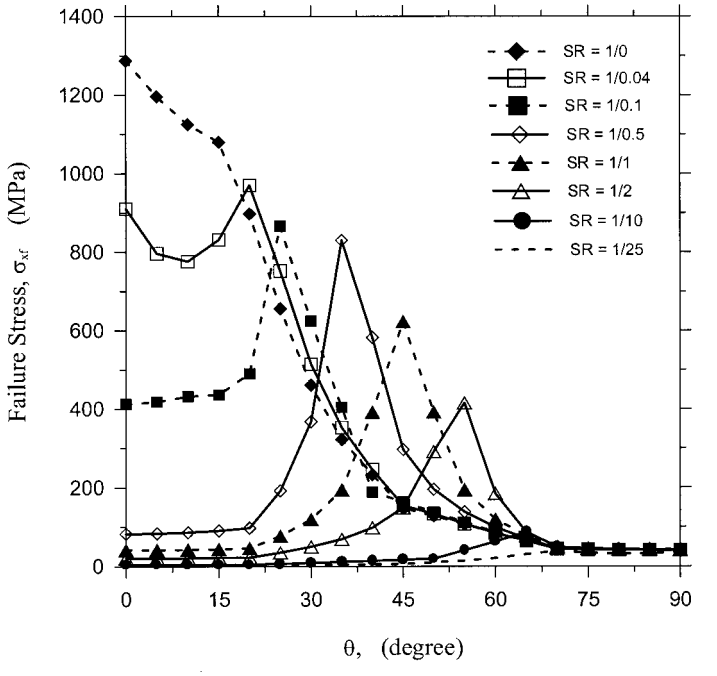

Figure 10. *Failure stresses* σ_{xf} *for various* $[+\theta/-\theta]_S$ *laminates under various biaxial tensile loads.*

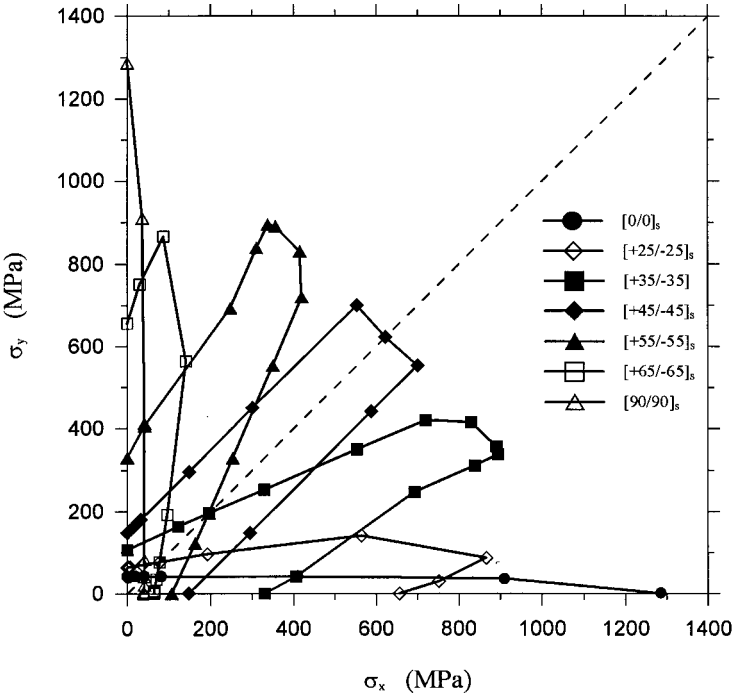

Figure 11. *Failure envelopes for various $[+\theta/-\theta]_S$ laminates under various biaxial tensile loads.*

decreasing of the biaxial stress ratio and the correspondent maximum axial failure stress decreases with the decreasing of the biaxial stress ratio. Figure 11 demonstrates the failure envelopes for various $[\pm\theta]_S$ laminates under different biaxial tensile loads. It is not surprising to find that the failure envelope of the $[\pm\theta]_S$ laminate is symmetric to that of the $[\pm(90-\theta)]_S$ laminate with the diagonal of the figure being the symmetric line.

$[\theta/(\theta-90)]_S$ LAMINATES

In this section, the influence of biaxial stress ratio on the stress–strain behavior of a given $[\theta/(\theta-90)]_S$ laminate is investigated. The laminates include $[0/90]_S$, $[+15/-75]_S$, $[+30/-60]_S$ and $[+45/-45]_S$ layups. Then, the influence of laminate layup on the stress–strain behaviors of various $[\theta/(\theta-90)]_S$ laminates under different biaxial stress ratios, i.e., $SR = 1/0$, $1/0.5$ and $1/1$, is studied. Finally, the influence of laminate layup on the failure stress and the failure envelope of various $[\theta/(\theta-90)]_S$ composite laminates under different biaxial stress is investigated.

Figures 12–14 and 8 illustrate the stress–strain curves for various $[\theta/(\theta-90)]_S$ laminates under different biaxial tensile loads. For $[0/90]_S$ laminate (Figure 12), the axial strains are positive for all loading conditions. The transverse strains are also positive except for $SR = 1/0$, which is due to the effect of the Poisson's ratio. Under the biaxial loading with SR changing from $1/0$ to $1/0.5$, the matrix cracking initiates on 90° ply (initial failure). Then matrix cracking occurs on 0° ply (intermediate failure). Finally fiber breaks on 0° ply (final failure). Under the equal biaxial loading, $SR = 1/1$, the matrix cracking initiates on 0 and 90° plies at the same time (initial failure) and finally fiber breaks on

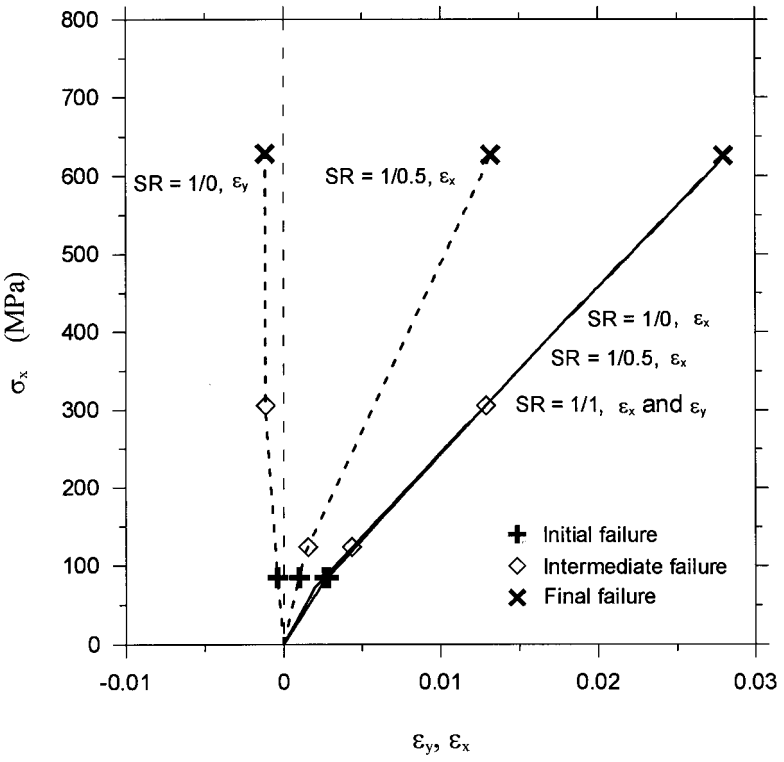

Figure 12. *Stress–strain curves for $[0/90]_S$ laminate under various biaxial tensile loads with SR = 1/0, 1/0.5 and 1/1.*

0 and 90° plies simultaneously (final failure). It appears that the initial failure stresses and the final failure stresses for all the loading conditions are the same. This is because the initial failure and final failure all occur in the 0 or 90° directions. The intermediate failure stress decreases as SR changes from 1/0 to 1/1 and no intermediate failure occurs as $SR = 1/1$.

For $[+15/-75]_S$ laminate (Figure 13), the trends of the stress–strain curves are similar to those of $[0/90]_S$ laminate. The failure propagation is similar to that of $[0/90]_S$ laminate with failures on 0 and 90° plies being converted to 15 and −75° plies, respectively. These curves have similar initial failure stresses with SR changing from 1/0 to 1/1. The final failure stress somewhat increases as SR changes from 1/0 to 1/1, due to the lateral tensile stress decreasing the axial strain to enhance the axial failure stress. The intermediate failure stress decreases as SR changes from 1/0 to 1/1, due to the incremental transverse stress causing the matrix cracking on 15° ply.

For $[+30/-60]_S$ laminate (Figure 14), the σ_x–ε_x and σ_x–ε_y curves are nonlinear under $SR = 1/0$, due to the laminate response dominated by shear deformation. The matrix-cracking initiates on −60° ply (initial failure). Then matrix cracking occurs on 30° ply (intermediate failure). Finally shear failure takes place simultaneously on 30 and −60° plies. For the biaxial loading with $SR = 1/0.5$, the initial matrix cracking occurs on −60° ply, followed by matrix cracking on 30° ply, and followed by shear failure on 30° ply. For the

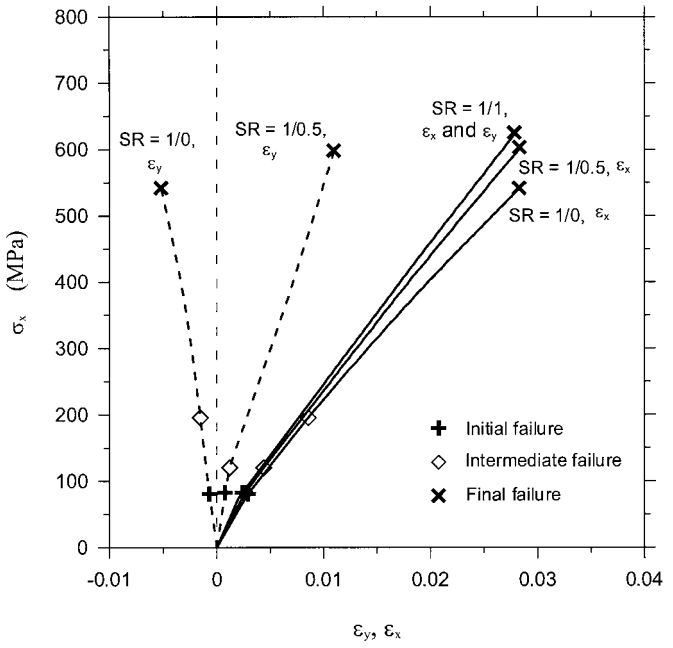

Figure 13. *Stress–strain curves for $[+15/-75]_S$ laminate under various biaxial tensile loads with SR = 1/0, 1/0.5 and 1/1.*

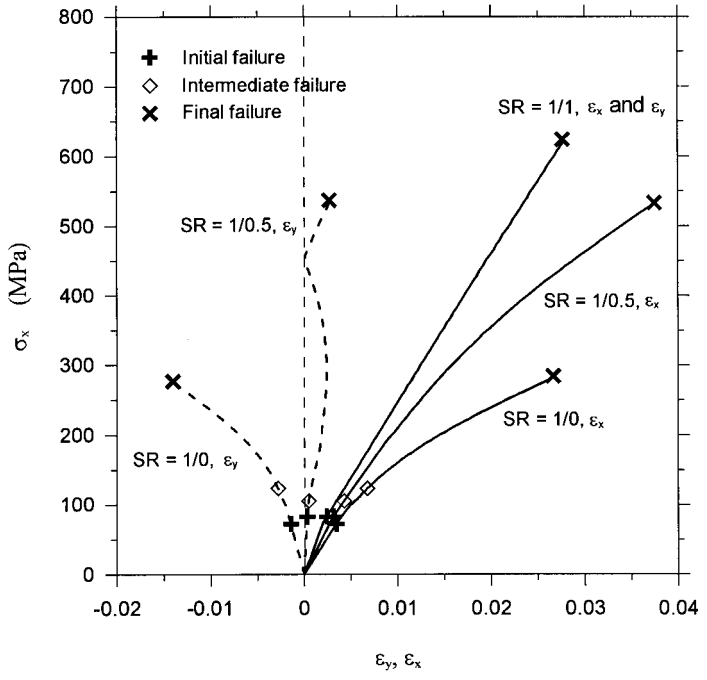

Figure 14. *Stress–strain curves for $[+30/-60]_S$ laminate under various biaxial tensile loads with SR = 1/0, 1/0.5 and 1/1.*

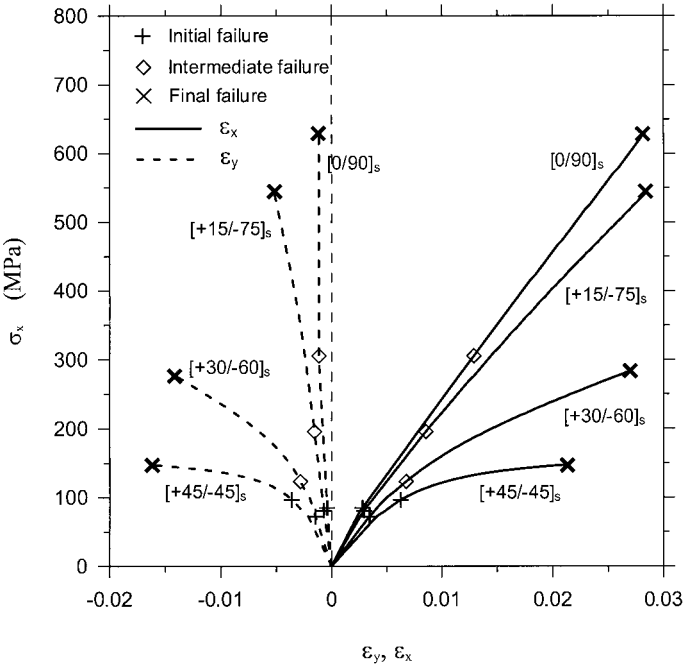

Figure 15. *Stress–strain curves for various $[\theta/(\theta-90)]_S$ laminates under biaxial tensile load with SR = 1/0.*

biaxial loading with $SR = 1/1$, the matrix cracking initiates on both 30 and -60° plies (initial failure). Finally, the fibers break on both 30 and -60° plies (final failure). It appears that the initial failure stresses for all the loading conditions are very similar. However, the final failure stress increases rapidly as SR changes from 1/0 to 1/1.

Figures 15–17 demonstrate the stress–strain curves for various $[\theta/(\theta - 90)]_S$ laminates under the certain biaxial tensile load. For uniaxial loading $SR = 1/0$ (Figure 15), the laminate response varies from fiber deformation dominated on $[0/90]_S$ layup to shear deformation dominated on $[+45/-45]_S$ layup. The laminates, except for $[+45/-45]_S$ laminate, experience initial matrix cracking on $(\theta - 90^\circ)$ ply, then followed by matrix cracking on θ ply, and finally followed by fiber breakage or shear failure on θ ply. The initial failure stresses are very close for various $[\theta/(\theta - 90)]_S$ laminates, but the intermediate and final failure stresses decrease rapidly as θ increases from 0 to 45°.

For the biaxial loading with $SR = 1/0.5$ (Figure 16), the axial and transverse strains are positive, except for $[+45/-45]_S$ laminate whose transverse strain changes from positive to negative. The laminate responses are dominated by fiber deformation on $[0/90]_S$ and $[+15/-75]_S$ layups, but dominated by shear deformation on $[+30/-60]_S$ and $[+45/-45]_S$ layups. The failure propagation is similar to the loading case for $SR = 1/0$. The initial and intermediate failure stresses are very close. That is, the occurrences of initial matrix cracking on $(\theta - 90^\circ)$ ply and the following matrix cracking on θ ply are very close. The final failure stress decreases as θ increases. As for the equal biaxial loading with $SR = 1/1$ (Figure 17), the axial and transverse strains are positive and all overlapped into the same curve for various $[\theta/(\theta - 90)]_S$ laminates. The behavior of this type of laminates is similar to the behavior of isotropic material under equal biaxial loading. So, it can be

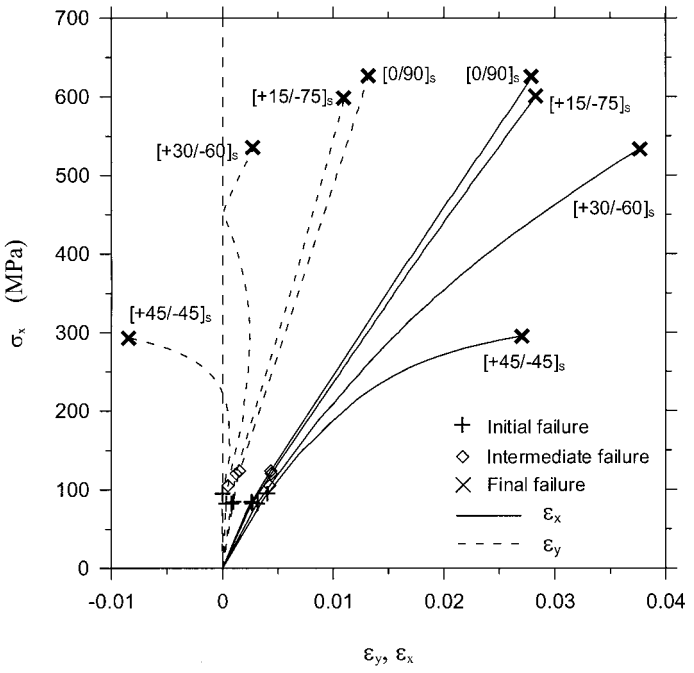

Figure 16. *Stress–strain curves for various $[\theta/(\theta - 90)]_S$ laminates under biaxial tensile load with SR = 1/0.5.*

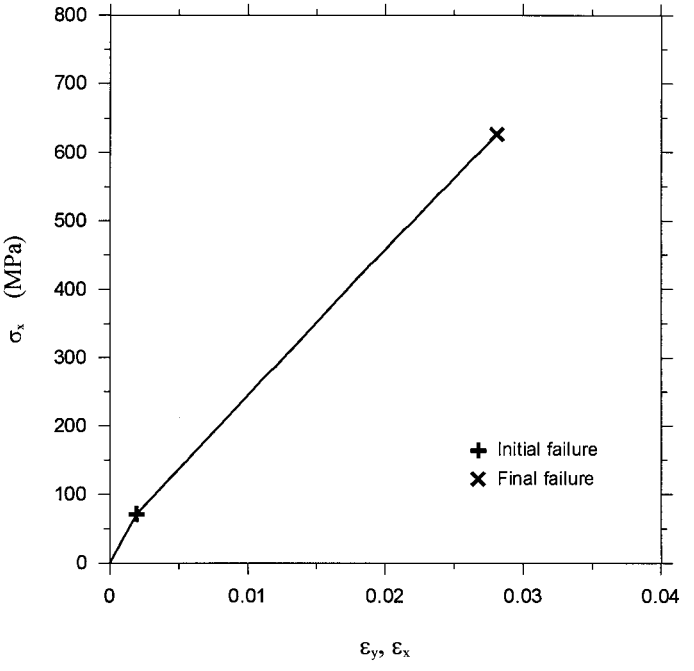

Figure 17. *Stress–strain curves for various $[\theta/(\theta - 90)]_S$ laminates under equal biaxial tensile load (SR = 1/1).*

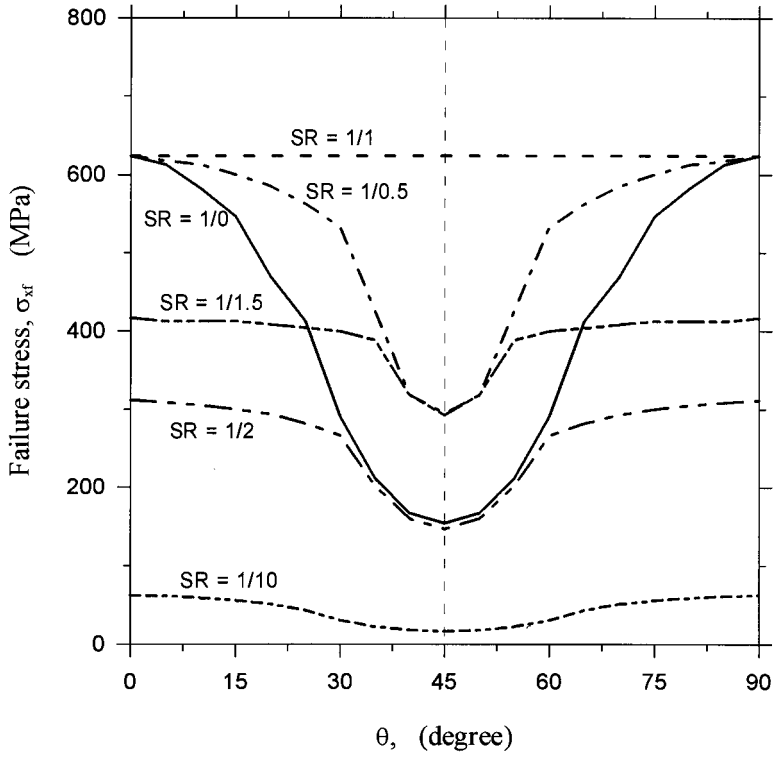

Figure 18. *Failure stresses σ_{xf} for various $[\theta/(\theta-90)]_S$ laminates under different biaxial tensile loads.*

referred to the conditional quasi-isotropic laminate. The laminates only experience initial matrix cracking on $(\theta-90^\circ)$ ply and finally fiber breakage on θ ply during the loading process.

Figure 18 illustrates the axial failure stresses for various $[\theta/(\theta-90)]_S$ laminates under different biaxial tensile loads. The $\sigma_{xf}-\theta$ curves are symmetric to the vertical line at $\theta=45^\circ$. The axial failure stress of $[\theta/(\theta-90)]_S$ laminates for all the biaxial loading conditions generally decreases as θ increases from 0 to 45°. The only exception is the case with $SR=1/1$, where the axial failure stress is a constant and independent of θ. Under the same θ angle, the axial failure stress increases with the decreasing of SR value when $1/1 \le \mathrm{SR} \le 1/0$. However, when $\mathrm{SR} \le 1/1$, the axial failure stress decreases with the decreasing of SR value. Comparing Figure 18 with Figure 10, we can see that the characteristic behaviors of $[\theta/(\theta-90)]_S$ laminate is greatly different from those of $[\pm\theta]_S$ laminate.

Figure 19 illustrates the failure envelopes for various $[\theta/(\theta-90)]_S$ laminates under different biaxial tensile loads. All the failure envelopes of the $[\theta/(\theta-90)]_S$ laminates are symmetric to the diagonal line of the figure. The shape of the failure envelope shrinks as θ increases from 0 to 45°. However, all curves pass through the same point on the diagonal line of the figure, where $SR=1/1$. It appears that the area of failure envelope for $[0/90]_S$ layup is the largest among various $[\theta/(\theta-90)]_S$ laminates under different biaxial loading. This means that the $[0/90]_S$ laminate can sustain the general biaxial loading more safely than the other $[\theta/(\theta-90)]_S$ laminates. Finally, the characteristic shapes of failure

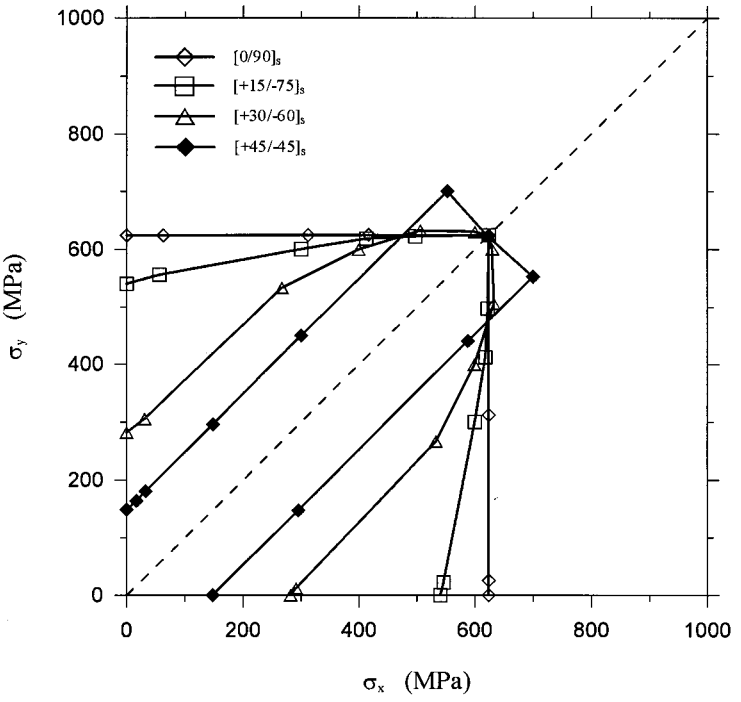

Figure 19. *Failure envelopes for various $[\theta/(\theta-90)]_S$ laminates under different biaxial tensile loads.*

envelopes for $[\theta/(\theta - 90)]_S$ laminates are also very different from those for $[\pm\theta]_S$ laminates as shown in Figure 11.

6. CONCLUSIONS

Based on the numerical investigation on the failure of composite laminates for various layups and under different biaxial loadings, the following conclusions can be drawn:

1. The proposed nonlinear failure analysis model can adequately predict the behavior of fiber-reinforced composite laminates under biaxial tensile loading The advantage of this analysis model includes its accuracy, ease of use, flexibility, scalar representation, and so on.
2. There are two major parameters, biaxial stress ratio and layup, which affect the behavior of the fiber-reinforced composite laminates under biaxial tensile stress. The $[\pm\theta]_S$ laminates have extremely distinct response from the $[\theta/(\theta - 90)]_S$ laminates under biaxial tensile loads, including the stress–strain behavior, failure stress-layup relation, and feature of failure envelope. There exists a symmetric condition on failure stress-layup relation with respect to $\theta = 45^\circ$ for $[\theta/(\theta - 90)]_S$ laminates, but it does not exist for $[\pm\theta]_S$ laminates.
3. The biaxial stress ratio affects the behavior of composite laminate not only on the failure stress but also on the failure mode. For $[\pm\theta]_S$ laminates, the maximum failure stress occurs at an optimum θ under a given biaxial stress ratio. The optimum θ

increases as the biaxial stress ratio, SR, decreases. The change of the biaxial stress ratio would change the failure mode of a laminate from one mode to another mode. For $[\theta/(\theta-90)]_S$ laminates, the maximum failure stress occurs on $[0/90]_S$ and $[90/0]_S$ layups under various biaxial stresses. However, under a special biaxial stress, the equal biaxial stress, the $[\theta/(\theta-90)]_S$ laminates would exhibit the same failure stress in spite of the θ angle. In general, the failure stress increases as the final failure mode of composite laminate changes from matrix cracking or shear failure dominant modes toward fiber failure dominant mode.

REFERENCES

1. Ellyin, F., Carroll, M., Kujawski, D. and Chiu, A.S. (1997). The behavior of multidirectional filament wound fibreglass/epoxy tubulars under biaxial loading. *Composites Part A*, **28A**: 781–790.
2. Soden, P.D., Kitching, R., Tse, P.C., Tsavalas, Y. and Hinton, M.J. (1993). Influence of winding angle on the strength and deformation of filament-wound composite tubes subjected to uniaxial and biaxial loads. *Composites Science and Technology*, **46**: 363–378.
3. Soden, P.D., Kitching, R. and Tse, P.C. (1989). Experimental failure stresses for $\pm 55^\circ$ filament wound glass fibre reinforced plastic tubes under biaxial loads. *Composites*, **20**(2): 125–135.
4. Al-Salehi, F.A.R., Al-Hassani, S.T.S. and Hinton, M.J. (1989). An experimental investigation into the strength of angle ply GRP tubes under high rate of loading. *J. Composite Materials*, **23**: 188–303.
5. Hull, D., Legg, M.J. and Spencer, B. (1978). Failure of glass/polyester filament wound pipe. *Composites*, **9**(1): 17–24.
6. Soden, P.D., Leadbetter, D., Griggs, P.R. and Eckold, G.C. (1978). The strength of a filament wound composite under biaxial loading. *Composites*, **9**: 247–250.
7. Gotsis, P.K., Chamis, C.C. and Minnetyan, L. (1998). Prediction of composite laminate fracture: micromechanics and progressive fracture. *Composites Science and Technology*, **58**(7): 1137–1149.
8. Eckold, G.C. (1998). Failure criteria for use in the design environment. *Composites Science and Technology*, **58**(7): 1095–1105.
9. Edge, E.C. (1998). Stress based Grant-Sanders method for predicting failure of composite laminates. *Composites Science and Technology*, **58**(7): 1033–1041.
10. McCartney, L.N. (1998). Predicting transverse crack formation in cross-ply laminate. *Composites Science and Technology*, **58**(7): 1069–1081.
11. Hart-Smith, L.J. (1998). Predictions of the original and truncated maximum-strain failure modes for certain fibrous composite laminates. *Composites Science and Technology*, **58**(7): 1151–1178.
12. Rotem, A. (1998). Prediction of laminate failure with the Rotem failure criterion. *Composites Science and Technology*, **58**(7): 1083–1094.
13. Sun, C.T. and Tao, J.X. (1998). Prediction of failure envelopes and stress/strain behaviour of composite laminates. *Composites Science and Technology*, **58**(7): 1125–1136.
14. Liu, K.-S. and Tsai, S.W. (1998). A progressive quadratic failure criterion of a laminate. *Composites Science and Technology*, **58**(7): 1023–1032.
15. Wolfe, W.E. and Butalia, T.S. (1998). A strain-energy based failure criterion for non-linear analysis of composite laminates subjected to biaxial loading. *Composites Science and Technology*, **58**(7): 1107–1124.
16. Zinoviev, P., Grigoriev, S.V., Labedeva, O.V. and Tairova, L.R. (1998). Strength of multilayered composites under plane stress state. *Composites Science and Technology*, **58**(7): 1209–1223.

17. Lin, W.-P. and Hu, H.-T. Nonlinear analysis of fiber-reinforced composite laminates subjected to uniaxial tensile load. *Journal of Composite Materials*. in press.
18. Hahn, H.T. and Tsai, S.W. (1973). Nonlinear elastic behavior of unidirectional composite laminates. *Journal of Composite Materials*, **7**: 102–118.
19. Mindlin, R.D. (1951). Influence of rotator inertia and shear flexural motions of isotropic elastic plate. *J. Appl. Mech.*, **18**: 31–38.
20. Narayanaswami, R. and Adelman, H.M. (1977). Evaluation of the tensor polynomial and Hoffman strength theories for composite materials. *Journal of Composite Materials*, **11**: 366–377.
21. Petit, P.H. and Waddoups, M.E. (1969). A method of predicting the nonlinear behavior of laminated composites. *Journal of Composite Materials*, **3**: 2–19.
22. Vaziri, R., Olson, M.D. and Anderson, D.L. (1991). A plasticity-based constitutive model for fibre-reinforced composite laminates. *Journal of Composite Materials*, **25**: 512–535.
23. Hu, H.-T. (1993). Influence of in-plane shear nonlinearity on buckling and postbuckling responses of composite laminate plates and shells. *Journal of Composite Materials*, **27**: 138–151.
24. Hibbitt, Karlsson & Sorensen, Inc. (2000). *ABAQUS Theory Manual and User Manual*, Version 5.8. Rhode Island: Providence.
25. Soden, P.D., Hinton, M.J. and Kaddour, A.S. (1998). Laminate properties lay-up configurations and conditions for a range of fibre-reinforced composite laminates. *Composites Science and Technology*, **58**(7): 1011–1022.